GDCh

Research Articles

Angewandte
Chemie
International Edition
www.angewandte.org

VIP | **Stereochemistry** | *Very Important Paper*

Enantioselective Synthesis of Enantioisotopomers with Quantitative Chiral Analysis by Chiral Tag Rotational Spectroscopy

Mitchell D. Mills[+], Reilly E. Sonstrom[+], Zoua Pa Vang[+], Justin L. Neill, Haley N. Scolati, Channing T. West, Brooks H. Pate,* and Joseph R. Clark*

Abstract: Fundamental to the synthesis of enantioen-riched chiral molecules is the ability to assign absolute configuration at each stereogenic center, and to determine the enantiomeric excess for each compound. While determination of enantiomeric excess and absolute configuration is often considered routine in many facets of asymmetric synthesis, the same determinations for enantioisotopomers remains a formidable challenge. Here, we report the first highly enantioselective metal-catalyzed synthesis of enantioisotopomers that are chiral by virtue of deuterium substitution along with the first general spectroscopic technique for assignment of the absolute configuration and quantitative determination of the enantiomeric excess of isotopically chiral molecules. Chiral tag rotational spectroscopy uses noncovalent chiral derivatization, which eliminates the possibility of racemization during derivatization, to perform the chiral analysis without the need of reference samples of the enantioisotopomer.

Introduction

Practical methods for the synthesis and characterization of enantioisotopomers, specifically those in which a carbon is chiral by virtue of deuterium substitution (Figure 1a), have eluded chemists since the first report of optical activity for an enantioisotopomer in 1949.[1] This exclusive class of precisely deuterated small molecules holds tremendous potential for applications across several scientific disciplines, especially chemistry and medicine. Given the importance of chiral recognition in medicine, the report by Belleau and Burba in 1961 that an enzyme displays a high degree of optical specificity between enantioisotopomers remains both significant and topical in research (Figure 1b).[2] Despite this discovery more than half a century ago, the full potential of enantioisotopomers is not being realized. However, since the arrival of the first FDA approved deuterated drug, Deutetrabenazine,[3] selectively deuterated small organic molecules have emerged as novel drug leads in the development of safer medicines.[4,5] Consequently, enantioisotopomers could play a role in future development of deuterated pharmaceuticals, where precise control of the deuteration pattern is increasingly desired.[6]

The intrinsically small differences among pairs of isotopically chiral molecules pushes the limits of both synthesis and spectroscopic analysis. Consequently, these chiral molecules have inspired impacting discoveries in asymmetric synthesis,[7,8] elucidation of enzymatic mechanisms,[9,10] polymer chemistry,[11,12] and spectroscopy.[13–18] Furthermore, understanding the origin of biological homochirality remains at the forefront of scientific research,[19] and the experimental observation that enantioisotopomers induce asymmetric autocatalysis in the Soai reaction may imply that enantioisotopomers have a larger role to play in chemical research beyond serving as tools to advance reactions, techniques, or mechanistic understanding.[8,20–22]

Despite the tremendous potential that enantioisotopomers have in chemical research, no general and highly selective protocols exist for their synthesis. The challenges facing synthetic chemists in the preparation and characterization of enantioisotopomers is highlighted over several decades in the pursuit of making (*S*)-ethylbenzene-*d1*, the benchmark sample used in this study, in high enantiopurity (Figure 1c).[23–26] While some reports offer short, 2-step routes, they require an enantioenriched starting material, can be low yielding, and lack characterization data regarding enantiopurity and absolute stereochemistry.[23,25,26] Other reported routes to provide (*S*)-ethylbenzene-*d1* in an assumed high enantiopurity require a 7-step synthesis and an enantioenriched starting material.[24,27,28]

The synthetic challenges described in the preparation of enantioisotopomers with high enantioenrichment are compounded by a lack of analytical chemistry techniques for establishing the absolute configuration (AC) at the stereogenic center and measuring the enantiomeric excess (EE)

[*] M. D. Mills,[+] Z. P. Vang,[+] Prof. Dr. J. R. Clark
Department of Chemistry, Marquette University
Milwaukee, WI 53233 (USA)
E-mail: joseph.r.clark@marquette.edu

Dr. R. E. Sonstrom,[+] H. N. Scolati, C. T. West, Prof. Dr. B. H. Pate
Department of Chemistry, University of Virginia
Charlottesville, VA 22904 (USA)
E-mail: bp2k@virginia.edu

Dr. J. L. Neill
BrightSpec Inc.
770 Harris Street Suite 104b, Charlottesville, VA 22903 (USA)

[+] These authors contributed equally to this work.
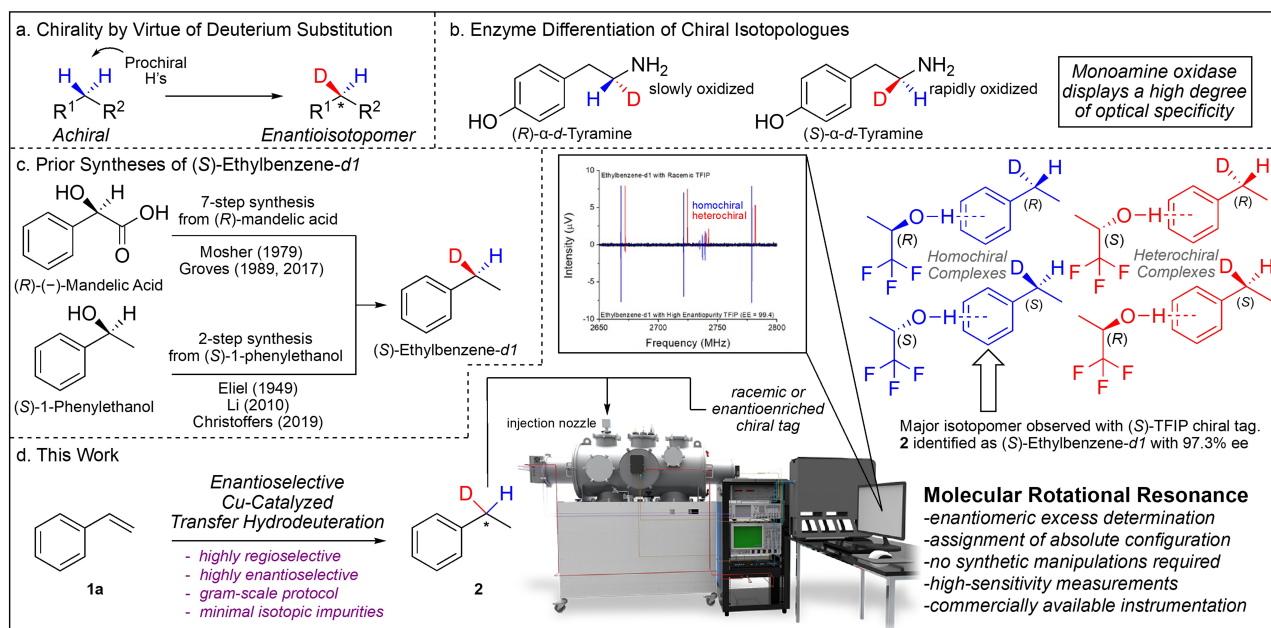
Figure 1. Synthesis and spectroscopic analysis of enantioisotopomers that are chiral by virtue of deuterium substitution. [a] A molecule containing a prochiral methylene site becomes chiral when a hydrogen is replaced with a deuterium. [b] Enzymes display a high degree of optical specificity in certain molecules containing a single stereogenic center that is chiral by virtue of deuterium substitution. [c] All prior syntheses of (*S*)-ethylbenzene-*d1* require a chiral starting material and multi-step synthetic route. Absolute determination of enantiomeric excess (EE) has only been achieved by Christoffers in 2019 by NMR spectroscopy after a multi-step synthetic derivatization. [d] This work demonstrates a Cu-catalyzed transfer hydrodeuteration for the enantioselective synthesis of (*S*)-ethylbenzene-*d1* in one-step, using an abundant achiral alkene starting material. In total, three enantioselective Cu-catalyzed transfer hydrodeuterations are reported, with each product being analyzed by molecular rotational resonance spectroscopy for absolute determination of EE and absolute configuration (AC). This work also establishes chiral tagging in molecular rotational resonance (MRR) spectroscopy as the first general spectroscopic technique for the absolute determination of EE and AC of enantioisotopomers. In the gas phase, a chiral tag binds to the analyte and creates a diastereomeric mixture of isotopomers that are distinguishable by MRR. Analysis of each unique spectral signature permits determination of EE and AC.

of the sample. Direct liquid chromatographic separation of enantiomers that are chiral by virtue of deuterium substitution has been demonstrated for a small number of analytes containing a highly deuterated phenyl substituent.[29,30] However, these separations are time consuming, and the AC can only be established through comparisons between retention times of structurally similar analytes requiring additional synthetic work. Two approaches with nuclear magnetic resonance (NMR) spectroscopy have been used to measure the EE of enantioisotopomers: chiral derivatization and deuterium quadrupole structure of molecules aligned in chiral media.[13,26,31,32] Chiral derivatization approaches require molecule-specific development of the derivatizing agent as illustrated by a previous analysis of ethylbenzene-*d1*.[26] Both chiral derivatization and ^{2}H-NMR measurements in aligned media pose challenges for high-confidence AC determination. For example, strong temperature dependence of the deuterium quadrupole splitting in aligned media—including reversal of the enantiomer signatures—has been noted.[13] Other techniques can be used to assign the AC of isotopically chiral molecules including routine laboratory techniques like vibrational circular dichroism (and the related technique of Raman optical activity)[17,33] and more complex emerging techniques like Coulomb explosion[16] that are not yet available for general analytical chemistry use.

Herein, we report the first metal-catalyzed, highly enantioselective synthesis of enantioisotopomers, along with the first general spectroscopic technique for absolute determination of EE and AC (Figure 1d). Analysis is performed using molecular rotational resonance (MRR) spectroscopy. The features of rotational spectroscopy and their utility in the analysis of the isotopologue and isotopomer composition of reaction mixtures of deuterated molecules, including the potential for high-throughput analysis, have been discussed in recent work.[34,35] The limitation that enantiomers of an isotopically chiral molecule have identical rotational spectra is addressed by employing the recently introduced chiral analysis method of chiral tag rotational spectroscopy.[36–38]

Results and Discussion

The unique strengths of rotational spectroscopy for isotope analysis are: 1) Each chemically distinct isotopic variant has a unique spectral signature. 2) The exceptionally high spectral resolution of MRR makes it possible to measure these spectra without overlap, so that complex isotopic mixtures can be analyzed without chromatographic separation (which is generally impossible for isotopic mixtures). 3) All isotopic species have the same equilibrium geometry,

and this geometry is used to calculate the transition frequencies for all isotopic variants. 4) The equilibrium geometry can be calculated to high accuracy by quantum chemistry, permitting high confidence identification of isotopic species without the need for reference compounds.

The focus of this work is the analysis of enantioisotopomers, which have identical rotational spectra at any practical spectral resolution.[39] In this case, MRR analysis occurs in the gas phase and uses noncovalent derivatization of the enantioisotopomers with a small chiral molecule of known configuration to produce distinguishable diastereomers. The chiral tag is added to the neon carrier gas used in the molecular beam experiments and attaches to the analyte during cluster formation in the pulsed jet expansion. Analysis of the spectra of these chiral tag complexes permits determination of both the AC and EE of the analyte.

This chiral tag analysis method is validated using samples of ethylbenzene-*d1* prepared by two literature methods. The first sample uses a synthetic route from Mosher and co-workers that was designed to ensure high enantiopurity and known AC of the prepared (*S*)-ethylbenzene-*d1* sample.[24] The second sample was prepared with the method developed by Christoffers and co-workers where they described a molecule-specific synthetic chiral derivatization method for NMR analysis finding EE = 92.[26]

The AC determination requires assigning a theoretical equilibrium geometry of the chiral tag complex to each observed rotational spectrum. The methodology used in this work uses a special feature of the analysis of enantioisotopomers. Under the Born-Oppenheimer approximation, all isotopic variants of the chiral tag complex have the same equilibrium geometry. As a result, the validation of the geometry can be performed using the normal isotopic species of the analyte (i.e., non-deuterated) which is generally available at lower cost.

The AC assignment for ethylbenzene-*d1* is made using 1,1,1-trifluoroisopropanol (TFIP) as the chiral tag, with the initial analysis using the normal species of ethylbenzene. TFIP was chosen because it has high volatility so that a gas mixture of the tag in the neon carrier gas can be prepared and because the large dipole moment of TFIP increases signal strength in the rotational spectrum of the tag complex. The equilibrium geometries for a set of candidate structures of the chiral tag complex are obtained from quantum chemistry to estimate the rotational constants that appear in the rigid rotor Hamiltonian for molecular rotation.[40] The calculated structures are reported in the Supporting Information. The theoretical rotational spectra of the complexes aid the analysis of the experimental spectrum. In general, several isomers of the tag complex are formed in the pulsed jet expansion and can be identified. The lowest energy structure for the ethylbenzene/TFIP complex is shown in Figure 2. Its calculated rotational constants are consistent with the experimental rotational constants of the highest intensity spectrum which are reported in Table 1 (as Isomer 1). The theoretical geometry is further validated by determining the positions of the carbon atoms in the complex using Kraitchman's method.[41] This analysis uses the assignment of the rotational spectra for the eleven singly
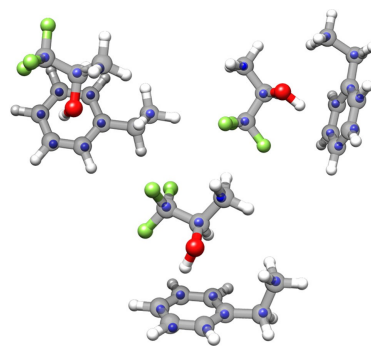
Figure 2. Three views of the lowest energy chiral tag complex formed between ethylbenzene and 1,1,1-trifluoroisopropanol are shown. The full structure is the equilibrium geometry obtained from quantum chemistry using the B2PLYPD3/def2TZVP model chemistry. This structure is validated by determining the positions of the carbon atoms using the assigned spectra for the 11 singly substituted ^{13}C isotopomers of the complex measured at natural abundance. These atom positions are shown by the smaller blue spheres superimposed on the quantum chemistry structure. The carbon atom position analysis validates the geometry of the chiral tag complex for the highest intensity spectrum, Isomer 1 of Table 1, observed in the measurement.

substituted ^{13}C-isotopomers of the complex observed in natural abundance. The details can be found in the Supporting Information. The experimental carbon atom positions are shown in Figure 2 as the blue spheres superimposed on the theoretical equilibrium geometry, showing excellent agreement.

The AC of ethylbenzene-*d1* is established in two steps as illustrated in Figure 3A, using a sample prepared by the Mosher route. The first measurement uses a racemic sample of the TFIP tag molecule to ensure that both homochiral and heterochiral complexes are formed regardless of the enantiopurity of the analyte. The homochiral and heterochiral designations use the Cahn-Ingold-Prelog labeling of the chiral centers in ethylbenzene-*d1* and TFIP. The ability to generate both diastereomers improves the confidence in assigning a spectrum to either the homochiral or heterochiral complex, as has been discussed for quantum chemistry-based diastereomer analysis by NMR spectroscopy.[42] A comparison of the theoretical rotational spectra of the homochiral and heterochiral complexes and experiment is shown in Figure 3A. The spectrum prediction uses the equilibrium geometry from quantum chemistry to obtain the rotational constants of each diastereomer. The predictions for each isotopomer are significantly improved scaling its calculated rotational constants by the ratio of the experimental and theoretical rotational constants of the normal species complex. The theoretical predictions are a close match to the experimental spectra, facilitating the assignment of the spectra for the homochiral and heterochiral tag complexes. The spectrum fit results are presented in Supporting Information. Using the assigned spectra, the deuterium atom position can be determined using Kraitchman's method. Kraitchman's method assumes an isotopically invariant molecular geometry and zero-point vibrational effects in C–H and C–D bonds can be expected to give

Table 1: Spectroscopic results used to establish the absolute configuration of the enantioisotopomers.

			Normal Species Chiral Tag Complex[a]					d1-Heterochiral		d1-Homochiral	
		Rotational Constant	Theory	Exp	Error [%]	Coordinate[b]		Theory	Exp	Theory	Exp
Ethylbenzene	Isomer 1	A [MHz]	836.2805	842.60004(2)	+0.75	|a| [Å]		3.849	3.731	4.034	4.082
		B [MHz]	389.1585	377.19543(1)	−3.17	|b| [Å]		1.558	1.596	1.598	1.673
		C [MHz]	320.6218	312.716200(9)	−2.53	|c| [Å]		1.214	1.430	0.529	0.316
	Isomer 2	A [MHz]	788.1058	786.34600(3)	−0.22	|a| [Å]		1.144	1.254	0.736	0.495
		B [MHz]	388.0129	384.433110(9)	−0.93	|b| [Å]		2.072	2.030	2.336	2.443
		C [MHz]	324.3261	321.904190(9)	−0.75	|c| [Å]		1.482	1.524	0.203	[0][c]
2-Ethylnaphthalene	Isomer 1	A [MHz]	418.0842	414.112380(64)	−0.96	|a| [Å]		0.056	[0][c]	0.818	1.079
		B [MHz]	352.6475	351.472620(47)	−0.33	|b| [Å]		3.590	3.624	4.440	4.408
		C [MHz]	247.8086	247.272360(48)	−0.22	|c| [Å]		1.742	1.743	0.410	0.415
	Isomer 2	A [MHz]	428.5449	422.465040(63)	−1.44	|a| [Å]		3.973	3.700	2.813	2.765
		B [MHz]	334.0264	335.780650(59)	+0.52	|b| [Å]		2.567	2.790	2.555	2.681
		C [MHz]	242.0888	241.910620(49)	−0.07	|c| [Å]		0.491	0.431	1.808	1.785
3-Phenyl-1-propanol	Isomer 1	A [MHz]	757.6193	749.80158(18)	−1.04	|a| [Å]		1.048	1.192	0.386	0.587
		B [MHz]	598.8914	588.92377(10)	−1.69	|b| [Å]		2.395	2.349	1.408	1.352
		C [MHz]	414.6116	407.15502(10)	−1.83	|c| [Å]		1.843	1.850	1.744	1.697
	Isomer 2	A [MHz]	799.1322	802.90592(21)	+0.47	|a| [Å]		0.262	[0][c]	1.901	2.334
		B [MHz]	481.4207	468.04195(15)	−2.86	|b| [Å]		1.546	1.533	2.156	2.020
		C [MHz]	333.0144	326.033770(90)	−2.14	|c| [Å]		1.644	1.634	1.663	1.644

[a] The initial assignment of a calculated equilibrium geometry to an observed spectrum is made by comparing the experimental and theoretical rotational constants of the complex formed between the tag and the normal species of the analyte. The two highest intensity spectra are labelled Isomer 1 and Isomer 2. [b] The coordinates give the position of the hydrogen in the normal species chiral tag complex that undergoes deuterium substitution using the principal axis system for molecular rotation. Substitution at the two benzylic hydrogens will produce homochiral and heterochiral complexes, which can be differentiated by the position of the substituted hydrogen. The Kraitchman analysis only provides the magnitude of the coordinates so |a|, |b|, and |c| are the values reported. [c] The Kraitchman analysis assumes a rigid rotor molecule. Contributions from zero-point vibrational motion are present and can significantly affect the results when an atom coordinate is near zero. In these cases, the calculated atom coordinate squared is often a negative value. When this occurs, the coordinate is reported as [0] to denote a small coordinate where the position determination is dominated by the inertial defect from zero-point motion.

different average bond lengths. Experimental estimates show that the vibrationally averaged bond length differences are about 0.01 Å or less and are too small to affect the analysis conclusions.[43] This structural information is reported in Table 1 to support the identification of the homochiral and heterochiral chiral tag complexes. The results for the analysis of the second highest intensity spectrum of the ethylbenzene/TFIP complex are also reported in Figure 3A and in Table 1 (Isomer 2).

The second measurement uses a high enantiopurity sample of (*S*)-TFIP (EE = 99.4). The Mosher synthesis was designed to produce (*S*)-ethylbenzene-*d1* in high enantiopurity, so it is expected is that the homochiral spectra will be observed at higher signal levels. As seen in Figure 3A, this result is found for both isomers of the chiral tag complex. The full analysis, which includes precise structural information about the position of deuterium incorporation in two isomers of the chiral tag complexes to validate the quantum chemistry geometries (Table 1), provides a high-confidence assignment of the (*S*)-configuration in the Mosher ethylbenzene-*d1* sample.

The enantiomeric excess for ethylbenzene-*d1* is obtained from the ratio of the transition intensities for homochiral and heterochiral complexes. This method has been presented previously and so is only briefly described here.[36,38] The measurement uses transition intensities from the spectrum acquired using the racemic tag sample to correct

for the instrument response. The normalized transition intensities in the homochiral spectrum are defined as:

$$N_{Homochiral} = \frac{I_{enantiopure\ tag}}{I_{racemic\ tag}} \quad (1)$$

with a similar definition for the normalized heterochiral transition intensities. From any pair of homochiral and heterochiral transitions, the signal ratio, R, is defined as:

$$R = \frac{N_{Homochiral}}{N_{Heterochiral}} \quad (2)$$

This ratio is used to determine the enantiomeric excess through the expression:

$$\frac{R-1}{R+1} = \left(ee_{tag}\right)\left(ee_{analyte}\right) \quad (3)$$

where *ee* is the fractional enantiomeric excess for either tag or analyte (the usual percent enantiomeric excess, EE, is related to the fractional *ee* through: EE = *ee* × 100). The tag EE is known from separate calibration measurements. For EE determinations using broadband rotational spectra, the average value of the EE is determined from all possible
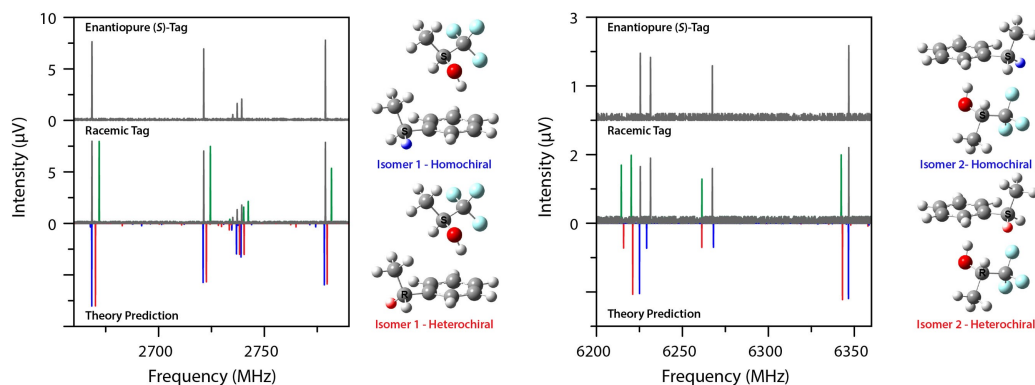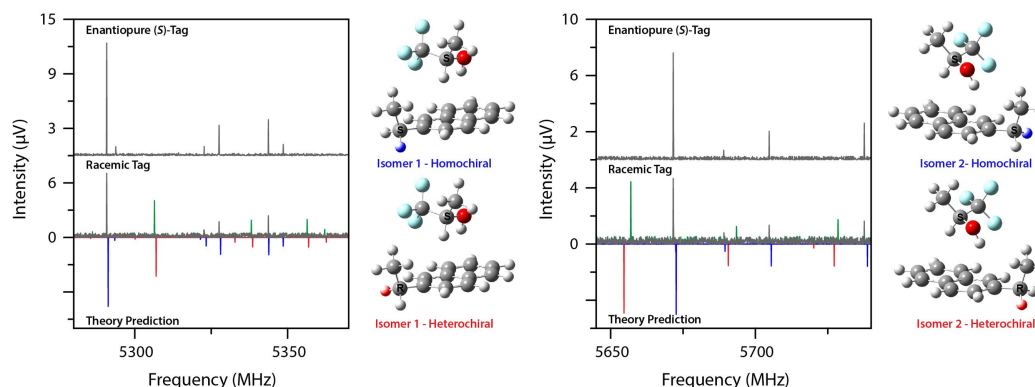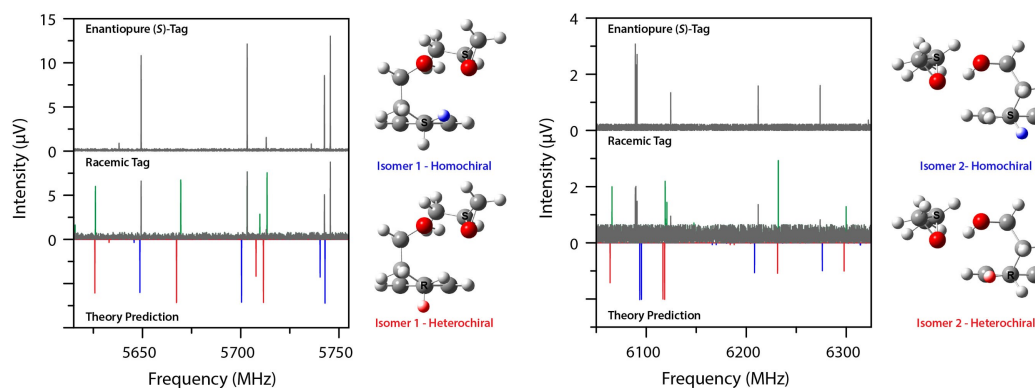
Figure 3. This figure illustrates how high-confidence assignment of the absolute configuration of the enantioisotopomers is made using MRR spectroscopy. The results for the sample prepared using the Mosher synthetic route, designed to give (S)-ethylbenzene-d1 in high enantiopurity, is shown in (A). The rotational spectra for the two diastereomer complexes of ethylbenzene-d1 with (S)-TFIP are calculated using the quantum chemistry equilibrium geometry. The structures for these complexes indicating the position of the deuterium substitution are shown to the right of the spectra. The left side panel in (A) shows the spectrum prediction using the theoretical structure of Figure 2. The right side gives the spectrum predictions using the structure assigned to the second highest intensity experimental spectrum (Isomer 2 of Table 1). The bottom part of the spectrum compares the theoretical spectra (negative going transitions, color coded blue for homochiral and red for heterochiral) to the measurement using racemic TFIP. These figures show only a small portion of the overall rotational spectrum which is recorded over the 2–8 GHz frequency range. The transitions associated with the two monomers, TFIP and ethybenzene-d1, have been cut from the experimental spectra for clarity. Spectra showing the full 2–8 GHz frequency range highlighting the assignments of the diastereomers for Isomer 1 and Isomer 2 can be found in Supporting Information. The experimental spectra are assigned based on the patterns predicted using the quantum chemistry structures. The black spectrum is for the homochiral complex and green is for heterochiral. These determinations are validated by comparing the atom position of deuterium substitution from Kraitchman analysis to the position in the quantum chemistry structure as listed in Table 1. Two isomers are analyzed to increase the confidence in the analysis. The top part of the spectrum shows the measurement using enantiopure (S)-TFIP (EE=99.4). This measurement is dominated by the spectrum of the homochiral tag complex for both chiral tag complex isomers confirming that the sample has high enantiopurity in (S)-ethylbezene-d1. The spectrum analyses for samples of 2-ethylnapthalene-d1 and 3-phenyl-1-propanol-d1 prepared using the new catalytic method are shown in (B) and (C), respectively. For phenylpropanol, the chiral tag is propylene oxide and the enantiopure tag measurement uses (S)-propylene oxide (EE=99.6). In both cases, the homochiral tag complex is dominant in the enantiopure tag measurement showing that these samples also have the (S)-configuration at the benzylic carbon and that the samples have high enantiopurity.

pairs of strong transitions in the homochiral and heterochiral spectra. The standard deviation of R is used to estimate the measurement uncertainty via the standard error.

The EE determination method is validated using a sample prepared following the synthetic route of Christoffers and co-workers, where the EE was determined by a chiral derivatization NMR method.[26] The chiral tag rotational spectroscopy measurement using this sample is shown in Figure 4A where a small spectral region of the enantiopure (S)-TFIP tag measurement is shown and compared to the result for the Mosher synthesis as well as the CuH synthesis discussed below. The key difference in these measurements is the observation of significant intensity in the heterochiral spectrum for the Christoffers sample, indicating a higher level of (R)-ethylbenzene-d1. A histogram of the EE determinations using all pairs of the 64 highest intensity transitions of the homochiral and heterochiral spectra is shown in Figure 4B. The chiral tag rotational spectroscopy result is EE = 85.7(3), where the value in parenthesis is the 1σ standard error in the units of the last decimal place. The reproducibility of the method was tested by performing three separate measurements over different days with results: 85.7(3), 85.4(3), 85.5(2). These results are reported in Supporting Information.

Validating the accuracy of the chiral tag method for applications to enantioisotopomers is difficult since there are no existing reference methodologies. We have made a test of the accuracy of Equation (3) over the full EE scale. A racemic sample of ethylbenzene-d1 was prepared using racemic starting materials in the Christoffers synthesis. The EE determination for this sample, EE = 1.2(6), is also shown in Figure 4B. A sample formed from a 2:1 mixture of the enantioenriched and racemic Christoffers samples was also analyzed. The gravimetric determination of the EE using the chiral tag rotational spectroscopy result for the enantioenriched sample is EE = 55. The chiral tag rotational spectroscopy determination shown in Figure 4B is in good agreement: EE = 57.0(3). The EE analysis of the two other ethylbenzene-d1 samples in this work are also shown in Fig 4B. The Mosher sample has EE = 98.6(1) and validates that this synthesis gives (S)-ethylbenzene-d1 in high enantiopurity. The (S)-ethylbenzene-d1 sample prepared by the new catalytic method reported in this work also has high enantiopurity, EE = 97.3(1).

Catalytic transfer hydrodeuteration reactions have unique advantages for the selective insertion of hydrogen (H) and deuterium (D) across a π-bond.[44] Recently, we reported the highest regioselectivities to date for an alkene transfer hydrodeuteration process, where a [Cu–H] species undergoes *syn*-addition across an alkene, followed by deuterodecupration.[35] We believe the observed regioselectivity is attributed to the high degree of catalyst control in the reaction, where the Cu species adds to the alkenyl carbon positioned α-to the arene, coupled with the H and D transfer reagents operating at distinct points in the reaction mechanism, which is consistent with other selective transfer hydrodeuteration processes.[45–49] With the groundwork laid for controlling regioselectivity in a Cu-catalyzed alkene transfer hydrodeuteration reaction, we hypothesized that the first metal-catalyzed enantioselective synthesis of an
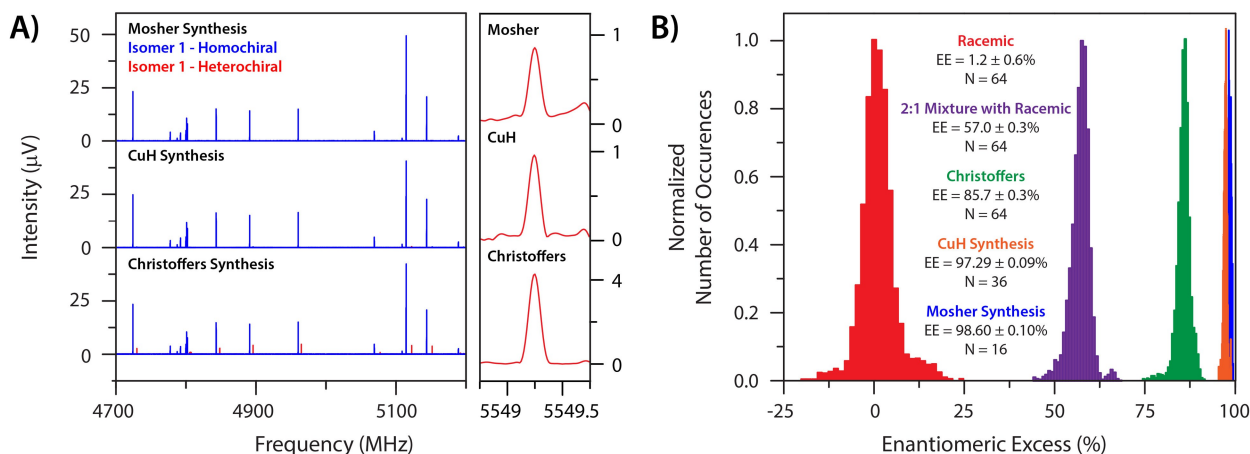
Figure 4. This figure shows the enantiomeric excess determinations for the three ethylbenzene-d1 samples used in the study. Part (A) shows the spectroscopic measurement using enantiopure (S)-TFIP tag for the three samples in a small frequency range of the full spectrum. The transitions associated with the heterochiral complex, which correlate to (R)-ethylbenzene-d1, are shown in red, but only easily visible in the Christoffers sample shown at the bottom. This indicates that the Christoffers synthesis produces a lower enantiopurity sample than either the Mosher synthesis (top and Figure 3A) or the new catalytic method introduced in this work (middle). An expanded scale view of the spectrum centered on one of the strongest transitions at about 5549 MHz is also shown and the heterochiral signals in the Mosher and CuH catalytic samples are clearly detected. The EE determination uses the statistics from all pairwise EE determinations using individual transitions from the homochiral and heterochiral spectra. The histograms showing the distribution of the pairwise EE values are shown in (B). Note that fewer transitions are used in the CuH (N = 36) and Mosher (N = 16) analyses due their higher enantiopurity compared to the Christoffers sample (N = 64). The mean and standard error for the EE determinations are reported in the legend of (B). Two additional measurements using the Christoffers synthetic route are shown to validate the EE determination. One uses racemic starting material and gives an EE = 1.2(6) which is close the expected EE = 0 value. The second measurement uses a 2:1 mixture of the enantioenriched Christoffers sample (EE = 85.7(3)) and the racemic preparation to give a sample with an estimated EE = 55. The experimental value, EE = 57.0(3), is in good agreement.

enantioisotopomer could be achieved if an appropriate chiral ligand was employed in the reaction. To test this hypothesis, we adopted reaction conditions similar to those reported by us in prior work,[35,50] and inspired by highly enantioselective processes for [Cu–H] catalyzed alkene hydrofunctionalizations,[51,52] we opted to employ (R)-DTBM-SEGPHOS as the ligand (EE = 99.9 from the manufacturer certificate of analysis). For the enantioselective synthesis of ethylbenzene-*d1*, 1 mol % of Cu(OAc)$_2$, 1.1 mol % of (R)-DTBM-SEGPHOS, polymethylhydrosiloxane (PMHS) and ethanol-OD were combined in THF in the presence of styrene **1a** (1 equiv) and stirred at room temperature for 16 h (Table 2). The reaction was performed on gram-scale and a 52 % yield of desired product **2** was isolated after purification. The absolute configuration and EE were determined using the chiral tag methodology described above, and isotopomer impurities such as a regioisomer arising from deuteration at the β-benzylic position were analyzed using the methods described in the previous work and found to be minimal (see Supporting Information for measurement details).[35] The sample is (S)-ethylbenzene-*d1* with EE = 97.3.

To evaluate if this protocol could be extended to other aryl alkene substrate types, we attempted the enantioselective transfer hydrodeuteration reaction with vinyl naphthalene substrate **1b** and isolated selectively deuterated product **3** in 78 % yield. After analysis using chiral tagging MRR spectroscopy, product **3** was determined to have EE = 97.7 and the S configuration was established at the stereogenic center. The spectroscopic analysis of the homochiral and heterochiral complexes between ethylnapthlanene-*d1* and TFIP is reported in Table 1. The chiral tag measurement

establishing the absolute configuration is shown in Figure 3B. That figure also shows the high enantiopurity of the sample through the much lower transition intensity of the heterochiral complex (i.e. (R)-ethylnapthlanene-*d1*/(S)-TFIP) in the measurement using high enantiopurity (S)-TFIP tag.

We also evaluated if this protocol could be extended to an internal alkene substrate type and subjected **1c** to enantioselective transfer hydrodeuteration conditions and isolated product **4** in 76 % yield (over 2-steps) after deprotection of the *tert*-butyldimethylsilane group. Although alcohol containing substrates do not inhibit reactivity in Cu-catalyzed transfer hydrogenation reactions,[53] a protecting group for the alcohol is required to avoid a competitive proto-decupration pathway. Analysis of **4** by MRR revealed the reaction to be highly enantioselective, EE = 98.1, leading to the S configuration at the stereogenic center. The spectroscopy analysis is presented in Table 1 with the measurement establishing absolute configuration shown in Figure 3C. In this case, propylene oxide was used as the tag molecule to make use of the strong hydrogen bond donor-acceptor interaction as shown in the structures of the tag complexes of Figure 3C. The very low transition intensity for the heterochiral tag complex spectrum when (S)-propylene oxide (EE = 99.6) is used as the tag shows that this substrate is also produced with high enantiopurity. The quantitative EE analysis of these three reaction products is presented in the Supporting Information.

Conclusion

In summary, a new synthetic methodology for the preparation of molecules where deuterium substitution creates a new chiral center is reported. The enantioselective Cu-catalyzed alkene transfer hydrodeuteration represents a one-step protocol to prepare highly enantioenriched molecules precisely deuterated at the α-benzylic position from readily available alkene substrates. The reaction can be performed on terminal or internal aryl alkenes and represents the first metal-catalyzed reaction for the enantioselective synthesis of enantioisotopomers. A full analysis of the isotopic composition of deuteration reaction products is possible using molecular rotational resonance spectroscopy. This work has demonstrated the use of chiral tag rotational spectroscopy for the analysis of enantioisotopomers. Both the assignment of absolute configuration and the measurement of the enantiomeric excess are accomplished without the need of any reference samples of the analyte. We note that a different approach to using MRR to perform chiral analysis—three-wave mixing rotational spectroscopy[54–56]—has recently been described for molecules that are chiral by virtue of deuteration. However, in its present state of development this technique cannot assign the AC of a sample because no method has been demonstrated that can determine the absolute phase of the chiral signal. Furthermore, the measurement of the EE requires a reference sample of known EE to calibrate the instrument. Ultimately, we anticipate the synthetic and spectroscopic advances

Table 2: Cu-catalyzed enantioselective alkene transfer hydrodeuteration reaction scope.
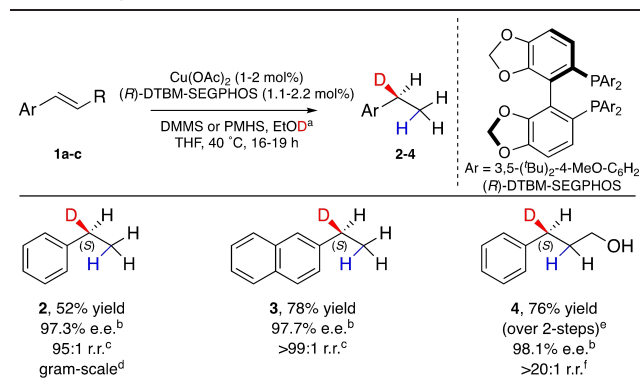
See Supporting Information for structures of compounds **1a–c**. [a] 4 equiv of dimethoxymethylsilane (DMMS) or poly(methylhydrosiloxane) (PMHS) along with 2.6 equiv of EtOD used in each reaction. [b] Enantiomeric excess (e.e.) was determined using chiral tagging in MRR spectroscopy. [c] The regioisomeric ratio (r.r.) was determined by MRR spectroscopy. [d] Reaction performed on gram scale using 11.5 mmol of styrene **1a**. [e] The 2-step yield includes the Cu-catalyzed transfer hydrodeuteration of **1c**, followed by removal of the TBS group using tetrabutylammonium fluoride (see Supporting Information for full experimental details). [f] The r.r. was determined using ¹H and ²H-NMR spectroscopy.

described will enable future precision deuteration reaction development and serve to expedite the use of enantioisotopomers as novel tools or molecule entities in high-impacting chemistry research.

Conflict of Interest

Authors Reilly Sonstrom, Justin Neill, and Brooks Pate have equity in BrightSpec, Inc., which commercializes MRR spectroscopy for analytical spectroscopy.

Data Availability Statement

All data supporting the findings of this study are available within the Article and its Supporting Information, or from the corresponding authors upon reasonable request.

[1] E. R. Alexander, A. G. Pinkus, *J. Am. Chem. Soc.* **1949**, *71*, 1786–1789.

[2] B. Belleau, J. Burba, M. Pindell, J. Reiffenstein, *Science* **1961**, *133*, 102–104.

[3] C. Schmidt, *Nat. Biotechnol.* **2017**, *35*, 493–494.

[4] T. Pirali, M. Serafini, S. Cargnin, A. A. Genazzani, *J. Med. Chem.* **2019**, *62*, 5276–5297.

[5] T. G. Gant, *J. Med. Chem.* **2014**, *57*, 3595–3611.

[6] B. Czeskis, C. S. Elmore, A. Haight, D. Hesk, B. D. Maxwell, S. A. Miller, T. Raglione, K. Schildknegt, J. F. Traverse, P. Wang, *J. Labelled Compd. Radiopharm.* **2019**, *62*, 690–694.

[7] A. Horeau, A. Nouaille, K. Mislow, *J. Am. Chem. Soc.* **1965**, *87*, 4957–4958.

[8] I. Sato, D. Omiya, T. Saito, K. Soai, *J. Am. Chem. Soc.* **2000**, *122*, 11739–11740.

[9] J. W. Cornforth, J. W. Redmond, H. Eggerer, W. Buckel, C. Gutschow, *Nature* **1969**, *221*, 1212–1213.

[10] J. Lüthy, J. Rétey, D. Arigoni, *Nature* **1969**, *221*, 1213–1215.

[11] M. M. Green, N. C. Peterson, T. Sato, A. Teramoto, R. Cook, S. Lifson, *Science* **1995**, *268*, 1860–1866.

[12] S. Cantekin, D. W. R. Balkenende, M. M. J. Smulders, A. R. A. Palmans, E. W. Meijer, *Nat. Chem.* **2011**, *3*, 42–46.

[13] A. Meddour, I. Canet, A. Loewenstein, J. M. Pechine, J. Courtieu, *J. Am. Chem. Soc.* **1994**, *116*, 9652–9656.

[14] V. Baillif, R. J. Robins, I. Billault, P. Lesot, *J. Am. Chem. Soc.* **2006**, *128*, 11180–11187.

[15] J. Haesler, I. Schindelholz, E. Riguet, C. G. Bochet, W. Hug, *Nature* **2007**, *446*, 526–529.

[16] P. Herwig, K. Zawatzky, M. Grieser, O. Heber, B. Jordan-Thaden, C. Krantz, O. Novotný, R. Repnow, V. Schurig, D. Schwalm, Z. Vager, A. Wolf, O. Trapp, H. Kreckel, *Science* **2013**, *342*, 1084–1086.

[17] A. Masarwa, D. Gerbig, L. Oskar, A. Loewenstein, H. P. Reisenauer, P. Lesot, P. R. Schreiner, I. Marek, *Angew. Chem. Int. Ed.* **2015**, *54*, 13106–13109; *Angew. Chem.* **2015**, *127*, 13298–13302.

[18] K. Maeda, D. Hirose, N. Okoshi, K. Shimomura, Y. Wada, T. Ikai, S. Kanoh, E. Yashima, *J. Am. Chem. Soc.* **2018**, *140*, 3270–3276.

[19] D. G. Blackmond, *Chem. Rev.* **2020**, *120*, 4831–4847.

[20] K. Soai, T. Shibata, H. Morioka, K. Choji, *Nature* **1995**, *378*, 767–768.

[21] T. Kawasaki, M. Shimizu, D. Nishiyama, M. Ito, H. Ozawa, K. Soai, *Chem. Commun.* **2009**, 4396–4398.

[22] N. A. Hawbaker, D. G. Blackmond, *ACS Cent. Sci.* **2018**, *4*, 776–780.

[23] E. L. Eliel, *J. Am. Chem. Soc.* **1949**, *71*, 3970–3972.

[24] R. L. Elsenbaumer, H. S. Mosher, *J. Org. Chem.* **1979**, *44*, 600–604.

[25] Y. Chen, W. L. Tang, J. Mou, Z. Li, *Angew. Chem. Int. Ed.* **2010**, *49*, 5278–5283; *Angew. Chem.* **2010**, *122*, 5406–5411.

[26] J. Küppers, R. Rabus, H. Wilkes, J. Christoffers, *Eur. J. Org. Chem.* **2019**, 2629–2634.

[27] J. T. Groves, P. Viski, *J. Am. Chem. Soc.* **1989**, *111*, 8537–8538.

[28] W. Liu, M.-J. Cheng, R. J. Nielsen, W. A. Goddard, J. T. Groves, *ACS Catal.* **2017**, *7*, 4182–4188.

[29] W. H. Pirkle, K. Z. Gan, *Tetrahedron: Asymmetry* **1997**, *8*, 811–814.

[30] K. Kimata, K. Hosoya, T. Araki, N. Tanaka, *Anal. Chem.* **1997**, *69*, 2610–2612.

[31] R. Berger, J. Courtieu, R. R. Gil, C. Griesinger, M. Köck, P. Lesot, B. Luy, D. Merlet, A. Navarro-Vázquez, M. Reggelin, U. M. Reinscheid, C. M. Thiele, M. Zweckstetter, *Angew. Chem. Int. Ed.* **2012**, *51*, 8388–8391; *Angew. Chem.* **2012**, *124*, 8512–8515.

[32] C. Aroulanda, P. Lesot, *Chirality* **2022**, *34*, 182–244.

[33] T. Miura, T. Nakamuro, Y. Nagata, D. Moriyama, S. G. Stewart, M. Murakami, *J. Am. Chem. Soc.* **2019**, *141*, 13341–13345.

[34] J. A. Smith, K. B. Wilson, R. E. Sonstrom, P. J. Kelleher, K. D. Welch, E. K. Pert, K. S. Westerndorff, D. A. Dickie, X. Wang, B. H. Pate, W. D. Harman, *Nature* **2020**, *581*, 288–293.

[35] Z. P. Vang, A. Reyes, R. E. Sonstrom, M. S. Holdren, S. E. Sloane, I. Y. Alansari, J. L. Neill, B. H. Pate, J. R. Clark, *J. Am. Chem. Soc.* **2021**, *143*, 7707–7718.

[36] B. H. Pate, L. Evangelisti, W. Caminati, Y. Xu, J. Thomas, D. Patterson, C. Perez, M. Schnell in *Chiral Analysis*, 2nd ed. (Eds.: P. L. Polavarapu), Elsevier, Amsterdam, 2018, pp. 679–729.

[37] J. L. Neill, A. V. Mikhonin, T. Chen, R. E. Sonstrom, B. H. Pate, *J. Pharm. Biomed.* **2020**, *189*, 113474.

[38] R. E. Sonstrom, J. L. Neill, A. V. Mikhonin, R. Doetzer, B. H. Pate, *Chirality* **2022**, *34*, 114–125.

[39] R. Berger, G. Laubender, M. Quack, A. Sieben, J. Stohner, M. Willeke, *Angew. Chem. Int. Ed.* **2005**, *44*, 3623–3626; *Angew. Chem.* **2005**, *117*, 3689–3693.

[40] W. Gordy, R. L. Cook, *Microwave Molecular Spectra*, 3rd ed., Wiley, Hoboken, **1984**.

[41] J. Kraitchman, *Am. J. Phys.* **1953**, *21*, 17–24.

[42] S. G. Smith, J. M. Goodman, *J. Am. Chem. Soc.* **2010**, *132*, 12946–12959.

[43] D. R. Lide, *J. Chem. Phys.* **1960**, *33*, 1519–1522.

[44] Z. P. Vang, S. J. Hintzsche, J. R. Clark, *Chem. Eur. J.* **2021**, *27*, 9988–10000.

[45] S. Kopf, F. Bourriquen, W. Li, H. Neumann, K. Junge, M. Beller, *Chem. Rev.* **2022**, *122*, 6634–6718.

[46] M. Espinal-Viguri, S. E. Neale, N. T. Coles, S. A. Macgregor, R. L. Webster, *J. Am. Chem. Soc.* **2019**, *141*, 572–582.

[47] J. C. L. Walker, M. Oestreich, *Org. Lett.* **2018**, *20*, 6411–6414.

[48] L. Li, G. Hilt, *Org. Lett.* **2020**, *22*, 1628–1632.

[49] L. Li, G. Hilt, *Chem. Eur. J.* **2021**, *27*, 11221–11225.

[50] A. Reyes, E. R. Torres, Z. P. Vang, J. R. Clark, *Chem. Eur. J.* **2021**, *27*, e202104340.

[51] R. Y. Liu, S. L. Buchwald, *Acc. Chem. Res.* **2020**, *53*, 1229–1243.

[52] H. Wang, S. L. Buchwald in *Organic Reactions, Vol. 100* (Ed.: S. Denmark), Wiley, Hoboken, **2020**, pp. 121–206.

[53] S. E. Sloane, A. Reyes, Z. P. Vang, L. Li, K. T. Behlow, J. R. Clark, *Org. Lett.* **2020**, *22*, 9139–9144.

[54] D. Patterson, M. Schnell, J. M. Doyle, *Nature* **2013**, *497*, 475–477.

[55] D. Patterson, J. M. Doyle, *Phys. Rev. Lett.* **2013**, *111*, 23008.

[56] L. Satterthwaite, C. Pérez, A. L. Steber, D. Finestone, R. L. Broadrup, D. Patterson, *J. Phys. Chem. A* **2019**, *123*, 3194–3198.